Engineering Structures 226 (2021) 111406

Contents lists available at ScienceDirect

Engineering Structures

journal homepage: www.elsevier.com/locate/engstruct

Strain monitoring based bridge reliability assessment using parametric Bayesian mixture model

Y.Q. Ni [a,*], R. Chen [a,b]

[a] Department of Civil and Environmental Engineering, The Hong Kong Polytechnic University, Hung Hom, Kowloon, Hong Kong, China
[b] School of Civil Engineering and Transportation, South China University of Technology, Tianhe, Guangzhou 510641, China

ARTICLE INFO

Keywords:
Bridge
Structural health monitoring (SHM)
Heterogeneous and multimodal data
Strain/stress distribution
Bayesian mixture distribution model
Conditional reliability index

ABSTRACT

Bridge condition assessment by use of structural health monitoring (SHM) data has been recognized as a promising approach towards the condition-based preventive maintenance. In-service bridges are normally subjected to multiple types of loads such as highway traffic, railway traffic, wind and thermal effect, resulting in heterogeneous and multimodal data structure of strain/stress responses. This study aims to develop an SHM-based bridge reliability assessment procedure in terms of parametric Bayesian mixture modelling. The parametric mixture model admits representation of multimodal structural responses, while the Bayesian paradigm enables both aleatory and epistemic uncertainties to be accounted for in modelling. By defining appropriate priors for the mixture parameters that are viewed as random variables to interpret the model uncertainty, an analytical form of the full conditional posteriors is derived. A Markov chain Monte Carlo (MCMC) algorithm in conjunction with Bayes factor is explored to determine the optimal model order and estimate the joint posterior of the mixture parameters. In full compliance with the Bayesian framework, a conditional reliability index is elicited with the parametric Bayesian mixture model by using the first-order reliability method. The estimated value of the reliability index, which serves as a quantitative measure of health condition for the in-service bridge, can be successively updated with the accumulation of monitoring data. The proposed method is exemplified by using one-year strain monitoring data acquired from the instrumented Tsing Ma Suspension Bridge, in which the evolution of the estimated reliability index is obtained.

1. Introduction

Large-scale bridges are vital components to the infrastructure system. As time goes, in-service bridges suffer from inevitable deterioration due to material aging, harsh operational environment, increasing traffic demands as well as extreme events such as earthquake, typhoon and vessel collision. The continuous deterioration, if not repaired or revamped, cumulates into damage and affects the structural performance to various degrees from non-optimal operation to catastrophic failure, resulting in great economic loss or even casualties. To ensure the serviceability and integrity of in-service bridges in their life cycle, efficient inspection and maintenance strategies need to be planned and implemented in an optimal sense that make best use of limited budget available.

Thanks to the significant advancement in sensing, signal processing, data transmission, data management and computing technologies over the past two decades, the application of structural health monitoring (SHM) technology to bridge structures has become increasingly popular [1–8]. By permanently deploying multiple types of sensing devices on bridges, the on-structure long-term SHM system enables to continuously acquire measurement data about the structural responses, external loadings and environmental effects in an automatic manner. Apparently, instrumentation with automatic SHM system acts as a beneficial complement to bridge inspection that needs neither access to the bridge nor cease of traffic service. Integrating the SHM technology into practice of bridge inspection and assessment offers an ideal solution to condition-based preventive or predictive maintenance of in-service bridges.

Due to the presence of uncertainties in response and load monitoring data, SHM-based methods for reliability assessment of bridge components/system have been developed in view of the ability to account for the randomness associated with load effect and resistance, leading to a more rational condition assessment [9–14]. In the execution of SHM-based reliability assessment, probability distribution models are required for depicting the random variables associated with load effect

* Corresponding author.
E-mail addresses: ceyqni@polyu.edu.hk (Y.Q. Ni), ranchen@scut.edu.cn (R. Chen).

https://doi.org/10.1016/j.engstruct.2020.111406
Received 4 May 2020; Received in revised form 9 August 2020; Accepted 4 October 2020
Available online 26 October 2020

and resistance. The standard distribution models (e.g., normal, lognormal, Weibull, and Gumbel) have been adopted in the aforementioned studies to describe the statistical characteristics of load- and resistance-related variables. These unimodal distribution models, however, fail to characterize some complicated distributional features such as multimodality, skewness, or asymmetry arising from real-world SHM data. In reality, in-service bridges are normally subjected to multiple loads such as highway traffic, railway traffic, monsoons, typhoons, thermal effect and their combinations, leading to heterogeneous structural responses with multimodality [13,15–17]. The conventional unimodal distribution models are often inadequate to characterize the multimodal structural responses in that they tend to yield biased model estimation.

Finite mixture modelling [18,19] is deemed as an ideal technique to capture the multimodal data structure. Through a finite number of weighted standard component densities (e.g. Gaussian component), the mixture distribution models can approach various irregular density shapes. In the context of SHM, researchers have made efforts to utilize finite mixture distributions to model the real datasets with heterogeneity. Nair and Kiremidjian [20] applied the Gaussian mixture distribution to model a set of group-shaped vibration signals for structural damage identification. Ni et al. [21] proposed a Weibull-normal mixture distribution to model SHM-derived stress spectrum for fatigue life assessment. Xia et al. [22] developed a reliability-based condition assessment procedure by combining the Weibull mixture distribution and the expectation maximization algorithm. Enright and OBrien [23] used bimodal distribution models to describe the gross vehicle weights and wheelbase data collected by weigh-in-motion (WIM) system instrumented on bridges. Farhidzadeh et al. [24] modelled two bunches of acoustic emission parameters by a two-component Gaussian mixture distribution in performing crack mode classification. Li et al. [25] adopted the Gaussian mixture distribution to model vehicle-induced cable tension ratio for condition assessment of bridge cables. The mixture distribution models adopted in the above studies were all explored in the context of classical frequentist probability, where the model parameters (e.g. component means, variances, and mixing weights) were treated as fixed quantities to be estimated and therefore, uncertainty in the model parameters arising from variability and error in the observed data as well as due to model imperfection couldn't be interpreted.

Bayesian inference provides a dedicated framework for statistical modelling of unknown data, in particular, the ability of interpreting uncertainty in model estimation [26]. Over the past decades, Bayesian methods have been developed for uncertainty quantification [27–29], model updating [30–32], modal identification [33–36], and vibration-based damage detection [36–40] of engineering structures. Zhang and Mahadevan [41] and Garbatov and Soares [42] adopted Bayesian inference to update the parameters of probability distributions in line with fatigue reliability assessment. Papadimitriou et al. [43] presented a Bayesian approach to updating robust reliability using structural test data. Beck and Au [44] proposed an improved Metropolis-Hastings algorithm for Bayesian updating of robust reliability. Der Kiureghian [45] proposed a Bayesian procedure to calculate predictive reliability index and the corresponding failure probability. Strauss et al. [46] provided a Bayesian approach to updating prediction functions in reliability assessment by using monitoring data and historical data knowledge. Ching and Leu [47] proposed a Bayesian updating procedure for reliability assessment using condition-state inspection data and fault-tree model. Zhu and Frangopol [48] adopted Bayesian updating for reliability assessment of a ship structure using SHM data. Ni et al. [49] combined Bayesian regression analysis and reliability principles to formulate an anomaly index for condition assessment of bridge expansion joints using SHM data.

The aim of this investigation is to develop an SHM-based bridge reliability assessment procedure in terms of parametric Bayesian mixture modelling. The unknown parameters in the Bayesian mixture model are treated as random variables rather than fixed quantities in the conventional (frequentist) probabilistic models, making the model uncertainty be explicitly interpreted. Both aleatory and epistemic uncertainties are thus accounted for in the modelling. To facilitate the subsequent derivation of an analytical expression of the conditional reliability index, the Gaussian (normal) distribution is adopted as component density in this study. By defining appropriate conjugate priors for the mixture parameters and introducing a component indicator in conformance with a multinomial distribution for allocating the observed data to different components, the Gibbs sampler in conjunction with Bayes factor is pursued to numerically estimate the posterior distributions of the mixture parameters and determine the optimal model order, where a scale reduction factor is utilized to diagnose convergence of the iteration process. Then, a conditional reliability index in full compliance with the Bayesian mixture model is explicitly elicited by means of the first-order reliability method (FORM). The derived conditional reliability index is a function of the uncertain model parameters; thus the estimate of the conditional reliability index reflects both the aleatory uncertainty and epistemic uncertainty depicted in the mixture model and can be updated with successively accumulated SHM data. The proposed procedure is exemplified through a case study using one-year strain monitoring data collected from the suspension Tsing Ma Bridge, in which the Bayesian mixture models for various bridge deck components and the evolution of the corresponding conditional reliability indices are obtained.

2. Parametric Bayesian mixture modelling

2.1. Finite mixture model

The general finite mixture distribution model has a parametric probability density function (PDF) which is the form of weighted sum of multiple component densities. Let $p(\cdot)$ denote the PDF of a random variable. Consider an independent random variable Y arising from the finite mixture distribution, with its PDF being expressed as

$$p(y) = \sum_{k=1}^{K} \omega_k f(y|\theta_k) \tag{1}$$

where $f(y|\theta_k)$ is the kth component density parameterized by θ_k; ω_k denotes the mixing weight of the kth component, satisfying $0 \le \omega_k \le 1$ and $\sum_{k=1}^{K}\omega_k = 1$; and K is the number of components (also termed as model order). In the Bayesian paradigm, ω_k represents the probability of an observation coming from the kth mixture component. In the present study, the Gaussian (normal) distribution ($\mathcal{N}$) is adopted as component density, hence it becomes a finite Gaussian mixture (FGM) model that can be expressed as

$$p(y) = \sum_{k=1}^{K} \omega_k \mathcal{N}\left(y|\mu_k, \sigma_k^2\right) \tag{2}$$

where $\theta_k = \{\mu_k, \sigma_k^2\}$ are the mean and variance of the kth Gaussian component. Let $\boldsymbol{\theta} = \{\boldsymbol{\omega}, \boldsymbol{\mu}, \boldsymbol{\Sigma}\}$ denote the entire set of unknown mixture parameters comprising the mixing weights $\boldsymbol{\omega} = \{\omega_1, \cdots, \omega_K\}$, the component means $\boldsymbol{\mu} = \{\mu_1, \cdots, \mu_K\}$ and the component variances $\boldsymbol{\Sigma} = \{\sigma_1^2, \cdots, \sigma_K^2\}$. The elements in the vector $\boldsymbol{\theta} = \{\omega_1, \cdots, \omega_K, \mu_1, \cdots, \mu_K, \sigma_1^2, \cdots, \sigma_K^2\}$ are treated as independent random variables that need to be estimated in the Bayesian paradigm.

The difficulty in estimating the mixture model is the uncertainty of allocating observations to a component. It is therefore necessary to introduce an uncertain component indicator $z_i = \{z_{i1}, \cdots, z_{iK}\}$ for each observation $y_i (i = 1, \cdots, N)$ [26,50], where z_{ik} is defined to be one or zero depending on whether y_i comes from the kth component

$$z_{ik} = \begin{cases} 1, & \textit{if } y_i \textit{ comes from the } k\textit{th component} \\ 0, & \textit{otherwise} \end{cases} \tag{3}$$

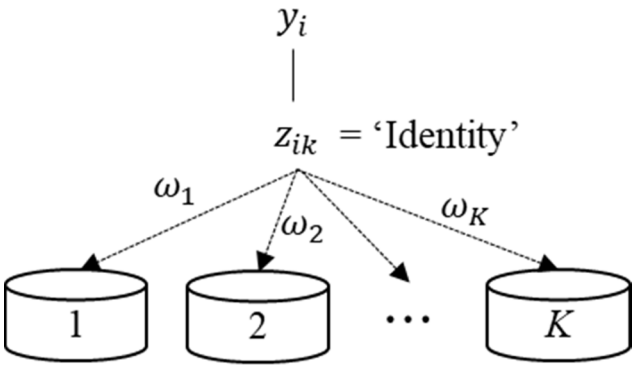

Fig. 1. Allocation of observations to each component.

A graphical illustration of the component indicator is depicted in Fig. 1. It follows that z_i conforms to a multinomial distribution (*Mult*)

$$z_i \sim Mult(1, \boldsymbol{\omega}) \tag{4}$$

and its probability mass function (PMF) can be expressed as

$$p(z_{i1}, \cdots, z_{iK}) = \frac{1!}{0!1!}\omega_1^{z_{i1}} \cdots \omega_K^{z_{iK}} = \omega_1^{z_{i1}} \cdots \omega_K^{z_{iK}} \tag{5}$$

Once the auxiliary variable z_i is sampled from the multinomial distribution, the allocation of each observation can be determined, and thus the parameters of each component distribution can be estimated accordingly. The overall unknown parameters in the FGM model are

$$\boldsymbol{\theta} = \{\omega_1, \cdots, \omega_K, \mu_1, \cdots, \mu_K, \sigma_1^2, \cdots, \sigma_K^2\} \text{ and } \boldsymbol{z} = \{z_1, \cdots, z_N\} \tag{6}$$

2.2. Selection of prior distributions

The Bayesian inference for the mixture model can be well defined once the prior distributions are appropriately determined [18]. The conjugate priors on the mixture parameters $\boldsymbol{\mu}$, $\boldsymbol{\Sigma}$ and $\boldsymbol{\omega}$ are adopted in the present study, because the use of conjugate priors allows the same distributional types for the posteriors of the model parameters as their priors and thus the obtained posteriors can be readily used as priors for updating the conditional reliability index when newly observed data are available. Integrals in posterior inference can be sidestepped by modifying the parameters in the prior distributions (so-called hyperparameters). For the mixture model, the full conditional posteriors can be explicitly derived if conjugate priors are adopted.

The component means and variances are assumed to be mutually independent over the components. Under this assumption, the scaled inverse-chi-square prior (*InvC*) and the normal prior can be used for σ_k^2 and μ_k [26,50]

$$\sigma_k^2 \sim InvC(\nu_k, s_k^2) \tag{7}$$

$$\mu_k|\sigma_k^2 \sim \mathcal{N}(\xi_k, \sigma_k^2/\kappa_k) \tag{8}$$

where $\{\nu_k, s_k^2\}$ and $\{\xi_k, \kappa_k\}$ are hyperparameters of the scaled inverse-chi-square density and the normal density for σ_k^2 and μ_k, respectively. The product of Eqs. (7) and (8) yields the joint prior distribution of $\theta_k = \{\mu_k, \sigma_k^2\}$, i.e., the normal-inverse-chi-square distribution, as

$$p(\mu_k, \sigma_k^2) \propto \sigma_k^{-1} (\sigma_k^2)^{-(\nu_k/2+1)} \exp\left(-\frac{\nu_k s_k^2 + \kappa_k(\mu_k - \xi_k)^2}{2\sigma_k^2} \right) \tag{9}$$

The mixing weights are assumed to be independent of the component means and variances. Thus, a suitable conjugate prior for $\boldsymbol{\omega}$ is the Dirichlet distribution (*Dir*) [18]

$$\boldsymbol{\omega} \sim Dir(\alpha_1, \cdots, \alpha_K) \tag{10}$$

which can be fully expressed as

$$p(\omega_1, \cdots, \omega_K) = \frac{\Gamma(\alpha_1 + \cdots + \alpha_K)}{\Gamma(\alpha_1) \cdots \Gamma(\alpha_K)} \omega_1^{\alpha_1 - 1} \cdots \omega_K^{\alpha_K - 1} \tag{11}$$

where α_k's are hyperparameters in the Dirichlet distribution, and $\Gamma(\cdot)$ denotes the gamma function.

2.3. Posterior distributions and Gibbs sampler

Given the observation data $\boldsymbol{y} = \{y_1, \cdots, y_N\}$, the joint posterior distribution of the mixture parameters can be obtained by applying Bayes' theorem

$$p(\boldsymbol{\theta}|\boldsymbol{y}, \boldsymbol{z}) = \frac{p(\boldsymbol{y}, \boldsymbol{z}|\boldsymbol{\theta}) p(\boldsymbol{\theta})}{\int p(\boldsymbol{y}, \boldsymbol{z}|\boldsymbol{\theta}) p(\boldsymbol{\theta}) \mathrm{d}\boldsymbol{\theta}} \tag{12}$$

where $p(\boldsymbol{\theta})$ is the joint prior distribution; and $p(\boldsymbol{y}, \boldsymbol{z}|\boldsymbol{\theta})$ is the likelihood function of the Gaussian mixture model in the following expression

$$p(\boldsymbol{y}, \boldsymbol{z}|\boldsymbol{\theta}) = p(\boldsymbol{z}|\boldsymbol{\omega}) p(\boldsymbol{y}|\boldsymbol{z}, \boldsymbol{\mu}, \boldsymbol{\Sigma}) = \prod_{i=1}^{N} \prod_{k=1}^{K} \left(\omega_k \mathcal{N}(y_i|\mu_k, \sigma_k^2) \right)^{z_{ik}} \tag{13}$$

and $\int p(\boldsymbol{y}|\boldsymbol{\theta}) p(\boldsymbol{\theta}) \mathrm{d}\boldsymbol{\theta}$ is the normalizing constant which is the integral over all possible values of the mixture parameters.

The direct inference of the joint posterior distribution using Eq. (12) is computationally intractable, especially when component number is large. In the past decades, various numerical algorithms based on Markov chain Monte Carlo (MCMC) simulation have been developed [26]. The basic idea behind MCMC-based algorithms is to generate a series of Markov chains from approximate distributions and then correct the samples so that the limiting distributions will approach the target distributions. The Gibbs sampler [51], one of the MCMC-based algorithms through full conditional sampling, is explored in this study to estimate the posterior distributions of the mixture parameters. Note that the introduction of $\boldsymbol{z}$ makes the mixture model a hierarchical conditional probability structure; therefore, one can effectively implement the Gibbs sampler as long as the full conditional posteriors can be articulated.

The implementation of the Gibbs sampler contains two major steps [26]: (i) sampling from the full conditional posterior distributions of the mixture parameters $\boldsymbol{\theta}$ given the current component indicators $\boldsymbol{z}$; and (ii) sampling from the full conditional posterior distribution of the component indicators $\boldsymbol{z}$ given the current mixture parameters $\boldsymbol{\theta}$. Given component indicators $\boldsymbol{z}$, say the allocation of observations is known at the moment, the Gaussian mixture model reduces to K independent Gaussian components in which each pair of Gaussian parameters μ_k and σ_k^2 can be estimated individually and straightforward. For the kth component, multiplying the joint prior distribution in Eq. (9) by the normal likelihood function yields the joint posterior distribution for $\theta_k = \{\mu_k, \sigma_k^2\}$ as

$$p(\mu_k, \sigma_k^2|\boldsymbol{y}_k, \boldsymbol{z}) \propto \sigma_k^{-1} (\sigma_k^2)^{-(\nu_k/2+1)} \exp\left(-\frac{\nu_k s_k^2 + \kappa_k(\mu_k - \xi_k)^2}{2\sigma_k^2} \right) \times (\sigma_k^2)^{-n_k/2} \exp\left(-\frac{1}{2\sigma_k^2} \left(\sum_{i \in k} \left(y_i - \bar{y}_k \right)^2 + n_k \left(\bar{y}_k - \mu_k \right)^2 \right) \right) \tag{14}$$

where $\boldsymbol{y}_k = \{y_i : z_{ik} = 1, i = 1 : N\}$ is the subset of $\boldsymbol{y}$ that contains the data points assigned to the kth component; n_k is the length of $\boldsymbol{y}_k$; and $\bar{y}_k$ is the sample mean of $\boldsymbol{y}_k$. Again Eq. (14) is the normal-inverse-chi-square distribution because of the conjugacy. The conditional posterior distribution of μ_k given σ_k^2 is proportional to the joint posterior distribution with σ_k^2 holding constant, which is the Gaussian density:

$$\mu_k|\sigma_k^2, \boldsymbol{y}_k, \boldsymbol{z} \sim \mathcal{N}(\xi_k^*, \sigma_k^2/\kappa_k^*) \tag{15}$$

where the hyperparameters ξ_k^* and κ_k^* are given by

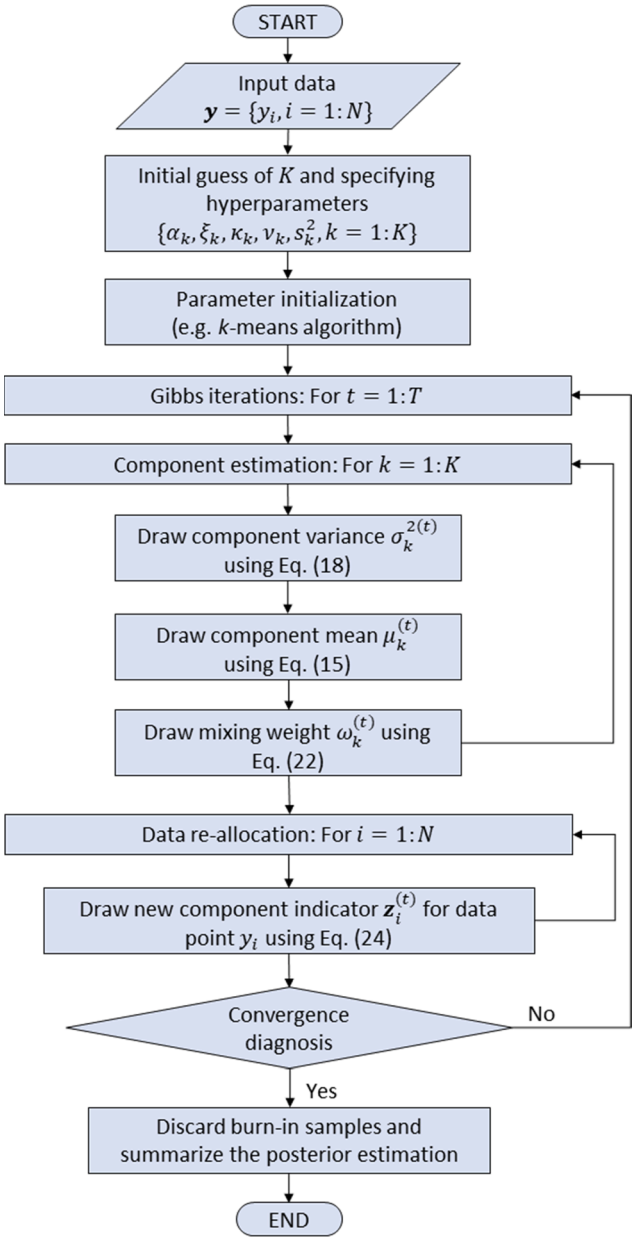

Fig. 2. Flowchart of Gibbs sampler for mixture model estimation.

$$\xi_k^* = \frac{\kappa_k \xi_k + n_k \bar{y}_k}{\kappa_k + n_k} \tag{16}$$

$$\kappa_k^* = \kappa_k + n_k \tag{17}$$

Then the marginal posterior distribution of σ_k^2 can be derived by integrating the joint posterior distribution over μ_k, which is the scaled inverse-chi-square density:

$$\sigma_k^2 | \boldsymbol{y}_k, z \sim InvC(\nu_k^*, s_k^{2*}) \tag{18}$$

where the hyperparameters ν_k^* and s_k^{2*} are given by

$$\nu_k^* = \nu_k + n_k \tag{19}$$

$$s_k^{2*} = \frac{1}{\nu_k + n_k}\left(\nu_k s_k^2 + \sum_{i \in k}\left(y_i - \bar{y}_k\right)^2 + \frac{\kappa_k n_k}{\kappa_k + n_k}\left(\bar{y}_k - \xi_k\right)^2\right) \tag{20}$$

The posterior distribution of the mixing weights $\boldsymbol{\omega}$ are derived using Bayes' theorem

$$p(\boldsymbol{\omega}|\boldsymbol{y}, z) \propto p(\boldsymbol{y}, z|\boldsymbol{\omega}) p(\boldsymbol{\omega}) = \omega_1^{n_1} \cdots \omega_K^{n_K} \times \omega_1^{\alpha_1 - 1} \cdots \omega_K^{\alpha_K - 1} = \prod_{j=1}^{J} \omega_j^{\alpha_j + n_j - 1} \tag{21}$$

which has exactly the form of the Dirichlet distribution. Thus, it can be expressed as

$$\boldsymbol{\omega}|\boldsymbol{y}, z \sim Dir(\alpha_1^*, \cdots, \alpha_K^*) \tag{22}$$

where the hyperparameter α_k^* is given by

$$\alpha_k^* = \alpha_k + n_k \tag{23}$$

Comparing the algebraic forms of the posterior distributions and the prior distributions on $\boldsymbol{\mu}$, $\boldsymbol{\Sigma}$ and $\boldsymbol{\omega}$, it is observed that the hyperparameters of the posteriors contain the information about both priors and observations.

Now we proceed to the posterior distribution of the component indicators z given mixture parameters $\boldsymbol{\theta}$. Eq. (4) tells that the distribution of z_i relies on the mixing weights which shall be updated once the mixture parameters are given. Thus, the posterior distribution of z_i for observation y_i can be expressed as

$$z_i | y_i, \boldsymbol{\omega}, \boldsymbol{\mu}, \boldsymbol{\Sigma} \sim Mult(1, \boldsymbol{\tau}_i) \tag{24}$$

where $\boldsymbol{\tau}_i = \{\tau_{i1}, \cdots, \tau_{iK}\}$ is the vector of updated mixing weights. The kth element τ_{ik} of $\boldsymbol{\tau}_i$ is the updated probability that y_i belongs to the kth component with y_i having been observed on it. By Bayes' theorem, it can be obtained as

$$\tau_{ik} = P(z_{ik} = 1 | y_i) = \frac{P(y_i | z_{ik} = 1) P(z_{ik} = 1)}{\sum_{k=1}^{K} P(y_i | z_{ik} = 1) P(z_{ik} = 1)} = \frac{\omega_k \mathcal{N}(y_i | \mu_k, \sigma_k^2)}{\sum_{k=1}^{K} \omega_k \mathcal{N}(y_i | \mu_k, \sigma_k^2)} \tag{25}$$

where $P(\cdot)$ denotes the probability of an event; and ω_k is viewed as the prior probability that y_i belongs to the kth component.

Having obtained the full conditional posterior distributions for all unknown parameters, the implementation procedures of Gibbs sampler for the Gaussian mixture model can be illustrated in Fig. 2. Repeating the process, say $t = 1, \cdots, T$, the Gibbs sampler proceeds with generating random samples successively from the full conditional posterior distributions and replacing the conditioning parameters. Early draws from the Gibbs sampler usually reflect the starting approximation rather than the target distributions. After discarding a certain number of early draws, referred to as burn-in samples B, the remaining $G = T - B$ random samples can be regarded as samples from the joint posterior distribution of the mixture parameters. With the generated posterior samples, the posterior distributions can be summarized, and the moments, quantiles and other statistic metrics of interest can be obtained. For instance, the most plausible mixture parameters can be estimated by the posterior sample means as

$$\widehat{\boldsymbol{\theta}} = G^{-1} \sum_{g=1}^{G} \boldsymbol{\theta}^{(g)} \tag{26}$$

where $\boldsymbol{\theta}^{(g)} (g = 1, \cdots, G)$ are the Gibbs outputs. Likewise, the parametric uncertainty can be characterized by the standard deviations (std) or credible intervals (CI) of the posterior samples. It should be noted that, to start the Gibbs sampler, a crude estimate of the initial values of z and $\boldsymbol{\theta}$ is needed. Here, the k-means algorithm [52] for parameter initialization is adopted in order to accelerate convergence of the Markov chains.

2.4. Quantitative convergence diagnosis

Convergence is of the highest concern when performing MCMC-based algorithms. Only when the Markov chain converges to the equilibrium distribution, the samples can then be representative of the target distribution, that is, the posterior distributions of the mixture

parameters in our case. Two practical tools have been widely used to examine the convergence issue. By displaying the iteration plots of the simulated Markov chains, one can perform visual inspection to check the convergence. It is commonly accepted that convergence is reached when the chain fluctuates within a certain region. Thus, longer iterations are needed to inspect the stationarity of the chain. Although the visual inspection is direct and easy to implement, it can be sometimes unreliable as subjective monitoring of convergence is still a puzzling task. Moreover, it fails to distinguish between local and global convergences in some cases [26].

Another way to diagnose convergence is using quantitative criteria. Based on the posterior sequences, the quantitative indicators tend to stabilize as the Markov chains converge. Gelman et al. [26] proved that the scale reduction factor R_0 as defined below is a good indicator for convergence diagnosis by comparing between- and within-sequence variances. It works with simultaneously running several parallel chains from dispersed starting points. Suppose several Markov chains (named parallel chains) of a mixture parameter θ are generated from randomly dispersed initial values, which are labelled as $\theta_q^{(t)}$ ($t = 1, \cdots, T$; $q = 1, \cdots, Q$) where T is the total number of iterations and Q is the number of parallel chains generated from different initial values. The scale reduction factor is calculated by

$$R_0 = \sqrt{\frac{T-1}{T} + \frac{V_b}{TV_w}} \tag{27}$$

where V_b is the between-sequence variance defined as

$$V_b = \frac{T}{Q-1}\sum_{q=1}^{Q}\left(\overline{\theta}_q - \overline{\theta}\right)^2 \tag{28}$$

with $\overline{\theta}_q = T^{-1}\sum_{t=1}^{T}\theta_q^{(t)}$ and $\overline{\theta} = Q^{-1}\sum_{q=1}^{Q}\overline{\theta}_q$; and V_w is the within-sequence variance defined as

$$V_w = \frac{1}{Q}\sum_{q=1}^{Q} s_q^2 \tag{29}$$

with $s_q^2 = \frac{1}{T-1}\sum_{t=1}^{T}(\theta_q^{(t)} - \overline{\theta}_q)^2$.

After sufficient iterations, the parallel chains would properly mix together, implying the chains converging to the same target distribution. As a result, the difference between V_b and V_w approaches a minimum, and the value of R_0 declines to 1 as $T \to \infty$. In this study, the convergence monitoring is performed by running two parallel chains for each parameter and convergence is reached when R_0 for all parameters drop to below 1.001.

2.5. Selection of optimal model order

The determination of optimal model order K in the mixture model is a model selection problem, which can be addressed by various model selection criteria. In the Bayesian paradigm, model comparison can be made by means of Bayes factor [19,26,53]. Suppose two competing models M_1 and M_2 are concerned, the Bayes factor (BF) is defined as

$$\mathrm{BF}(M_1;M_2) = \frac{p(y|M_1)}{p(y|M_2)} = \frac{\int p(y|\boldsymbol{\theta}_1, M_1)p(\boldsymbol{\theta}_1|M_1)\mathrm{d}\boldsymbol{\theta}_1}{\int p(y|\boldsymbol{\theta}_2, M_2)p(\boldsymbol{\theta}_2|M_2)\mathrm{d}\boldsymbol{\theta}_2} \tag{30}$$

where $p(\boldsymbol{y}|M_i) = \int p(\boldsymbol{y}|\boldsymbol{\theta}_i, M_i)p(\boldsymbol{\theta}_i|M_i)\mathrm{d}\boldsymbol{\theta}_i$ is the marginal likelihood (i.e., the normalizing constant) of model $M_i (i = 1, 2)$; $p(\boldsymbol{y}|\boldsymbol{\theta}_i, M_i)$ and $p(\boldsymbol{\theta}_i|M_i)$ are the likelihood function and prior density under model $M_i (i = 1, 2)$, respectively. If the observations $\boldsymbol{y}$ are more likely to come from model M_i, then the associated marginal likelihood $p(\boldsymbol{y}|M_i)$ will be larger, and vice versa. Thus, a Bayes factor $\mathrm{BF}(M_1;M_2) > 1$ implies that model M_1 is in favor of being more plausible than M_2 in featuring the observation data. In the case of multiple candidate models, e.g., the selection of optimal component number in a mixture model, it is usually more convenient to compare the logarithm of the marginal likelihood $\ln p(\boldsymbol{y}|M_i)$ (LML) of each model, then optimal model is the one with maximum LML value.

The calculation of the marginal likelihood $p(\boldsymbol{y}|M_i)$ which involves integration over high dimensional parameter space is in general analytically untraceable for complex models. A variety of numerical approximation algorithms have been developed for estimating marginal likelihood [19]. In this study, the marginal likelihood is estimated using Chib's method [53] which is based on the Gibbs outputs and Monte Carlo estimate. Recalling Eq. (12), the marginal likelihood can be rewritten as

$$p(\boldsymbol{y}|M_i) = \frac{p(\boldsymbol{y}|\boldsymbol{\theta})p(\boldsymbol{\theta})}{p(\boldsymbol{\theta}|\boldsymbol{y})} \tag{31}$$

in which the numerator is the product of the likelihood and prior density, and the denominator is the posterior density under model M_i. Note that this identity holds for any $\boldsymbol{\theta}$ and an efficient choice is using the posterior mean values $\widehat{\boldsymbol{\theta}}$ to estimate the marginal likelihood since the density functions have more accurate estimation at the large density points. As such, the LML evaluated at $\widehat{\boldsymbol{\theta}}$ is given by

$$\ln p(\boldsymbol{y}|M_i) = \ln p(\boldsymbol{y}|\widehat{\boldsymbol{\theta}}) + \ln p(\widehat{\boldsymbol{\theta}}) - \ln p(\widehat{\boldsymbol{\theta}}|\boldsymbol{y}) \tag{32}$$

The first two terms on the right-hand side of Eq. (32), i.e., the log likelihood and log prior density, can be readily evaluated by using the following expressions:

$$\ln p(\boldsymbol{y}|\widehat{\boldsymbol{\theta}}) = \sum_{i=1}^{N}\left(\ln\sum_{k=1}^{K}\widehat{\omega}_k N_k\left(y_i;\widehat{\mu}_k,\widehat{\sigma}_k^2\right)\right) \tag{33}$$

$$\begin{aligned}\ln p(\widehat{\boldsymbol{\theta}}) &= \ln p(\widehat{\boldsymbol{\Sigma}}) + \ln p(\widehat{\boldsymbol{\mu}}|\widehat{\boldsymbol{\Sigma}}) + \ln p(\widehat{\boldsymbol{\omega}}) \\ &= \sum_{k=1}^{K} lnp\left(\widehat{\sigma}_k^2\right) + \sum_{k=1}^{K} lnp\left(\widehat{\mu}_k|\widehat{\sigma}_k^2\right) + lnp(\widehat{\omega}_1, \cdots, \widehat{\omega}_K)\end{aligned} \tag{34}$$

where $\widehat{\boldsymbol{\mu}} = \{\widehat{\mu}_1, \cdots, \widehat{\mu}_K\}$, $\widehat{\boldsymbol{\Sigma}} = \{\widehat{\sigma}_1^2, \cdots, \widehat{\sigma}_K^2\}$ and $\widehat{\boldsymbol{\omega}} = \{\widehat{\omega}_1, \cdots, \widehat{\omega}_K\}$ are the posterior mean values of the mixture parameters $\boldsymbol{\mu}$, $\boldsymbol{\Sigma}$ and $\boldsymbol{\omega}$.

The third term on the right-hand side of Eq. (32) is the log posterior density which has implicit and high-dimensional form and cannot be calculated directly. As suggested by Chib [53], the joint posterior density can be factorized into the following three terms

$$\ln p(\widehat{\boldsymbol{\theta}}|\boldsymbol{y}) = \ln p(\widehat{\boldsymbol{\Sigma}}|\boldsymbol{y}) + \ln p(\widehat{\boldsymbol{\mu}}|\boldsymbol{y}, \widehat{\boldsymbol{\Sigma}}) + \ln p(\widehat{\boldsymbol{\omega}}|\boldsymbol{y}, \widehat{\boldsymbol{\mu}}, \widehat{\boldsymbol{\Sigma}}) \tag{35}$$

where each of these terms can be approximated by the Gibbs outputs. By running sufficient iterations of the Gibbs sampler for the so-called "first-phase simulation" where the full conditional distributions are $p(\boldsymbol{\mu}|\boldsymbol{y}, \boldsymbol{\Sigma}, z)$, $p(\boldsymbol{\Sigma}|\boldsymbol{y}, z)$, $p(\boldsymbol{\omega}|\boldsymbol{y}, z)$ and $p(z|\boldsymbol{y}, \boldsymbol{\omega}, \boldsymbol{\mu}, \boldsymbol{\Sigma})$, the approximate Monte Carlo estimate of the first term $p(\widehat{\boldsymbol{\Sigma}}|\boldsymbol{y})$ can be obtained as

$$p(\widehat{\boldsymbol{\Sigma}}|\boldsymbol{y}) = \int p(\widehat{\boldsymbol{\Sigma}}|\boldsymbol{y}, z)p(z|\boldsymbol{y})\mathrm{d}z \approx G_1^{-1}\sum_{g=1}^{G_1} p\left(\widehat{\boldsymbol{\Sigma}}|\boldsymbol{y}, z^{(g)}\right) \tag{36}$$

where $z^{(g)}$ are drawn from the distribution $p(z|\boldsymbol{y})$ corresponding to the first-phase Gibbs outputs of G_1 samples after discarding the burn-in samples. Then, set $\boldsymbol{\Sigma} = \widehat{\boldsymbol{\Sigma}}$ and run again iterations of the Gibbs sampler for the so-called "second-phase simulation" where the full conditional distributions are$p(\boldsymbol{\mu}|\boldsymbol{y}, \widehat{\boldsymbol{\Sigma}}, z)$, $p(\boldsymbol{\omega}|\boldsymbol{y}, z)$ and $p(z|\boldsymbol{y}, \boldsymbol{\omega}, \boldsymbol{\mu}, \widehat{\boldsymbol{\Sigma}})$. The Monte Carlo estimate of the second term $p(\widehat{\boldsymbol{\mu}}|\boldsymbol{y}, \widehat{\boldsymbol{\Sigma}})$ is given as

$$p(\widehat{\boldsymbol{\mu}}|\boldsymbol{y}, \widehat{\boldsymbol{\Sigma}}) = \int p(\widehat{\boldsymbol{\mu}}|\boldsymbol{y}, \widehat{\boldsymbol{\Sigma}}, z)p(z|\boldsymbol{y}, \widehat{\boldsymbol{\Sigma}})\mathrm{d}z \approx G_2^{-1}\sum_{g=1}^{G_2} p\left(\widehat{\boldsymbol{\mu}}|\boldsymbol{y}, \widehat{\boldsymbol{\Sigma}}, z^{(g)}\right) \tag{37}$$

where $z^{(g)}$ are drawn from the distribution $p(z|\boldsymbol{y}, \widehat{\boldsymbol{\Sigma}})$ corresponding to the second-phase Gibbs outputs of G_2 samples after discarding the burn-in samples. Lastly, set $\boldsymbol{\Sigma} = \widehat{\boldsymbol{\Sigma}}$ and $\boldsymbol{\mu} = \widehat{\boldsymbol{\mu}}$, and run again iterations of the

Gibbs sampler for the so-called "third-phase simulation" where the full conditional distributions are $p(\boldsymbol{\omega}|\boldsymbol{y},z)$ and $p(z|\boldsymbol{y},\boldsymbol{\omega},\widehat{\boldsymbol{\mu}},\widehat{\boldsymbol{\Sigma}})$. The Monte Carlo estimate of the third term $p(\widehat{\boldsymbol{\omega}}|\boldsymbol{y},\widehat{\boldsymbol{\mu}},\widehat{\boldsymbol{\Sigma}})$ is given as

$$p(\widehat{\boldsymbol{\omega}}|\boldsymbol{y},\widehat{\boldsymbol{\mu}},\widehat{\boldsymbol{\Sigma}}) = \int p(\widehat{\boldsymbol{\omega}}|\boldsymbol{y},z)p(z|\boldsymbol{y},\widehat{\boldsymbol{\mu}},\widehat{\boldsymbol{\Sigma}})\mathrm{d}z \approx G_3^{-1}\sum_{g=1}^{G_3} p(\widehat{\boldsymbol{\omega}}|\boldsymbol{y},z^{(g)}) \tag{38}$$

where $z^{(g)}$ are drawn from the distribution $p(z|\boldsymbol{y},\widehat{\boldsymbol{\mu}},\widehat{\boldsymbol{\Sigma}})$ corresponding to the third-phase Gibbs outputs of G_3 samples after discarding the burn-in samples. Substituting the estimates from Eqs. (36) to (38) into Eq. (35) yields the joint posterior density evaluated at $\widehat{\boldsymbol{\theta}}$. Together with Eqs. (33) and (34), the LML of model M_i can be calculated by Eq. (32).

3. Reliability assessment with Bayesian mixture model

3.1. Conditional reliability index

Given structural resistance R and load effect S, the limit state function for reliability analysis can be defined as [54]

$$h(\boldsymbol{X}) = R - S \tag{39}$$

where $\boldsymbol{X} = \{R,S\}$ are the basic random variables with respect to the structural resistance and load effect. $h = 0$ denotes the limit state, while $h < 0$ denotes the failure state. When the PDFs of the structural resistance and load effect are formulated by Bayesian inference using monitoring or test data, the uncertainties associated with R and S are accounted for through uncertain model parameters $\boldsymbol{\Theta} = \{\boldsymbol{\theta}_R,\boldsymbol{\theta}_S\}$ embedded in the limit state function:

$$h(\boldsymbol{X},\boldsymbol{\Theta}) = R - S \tag{40}$$

Then the failure probability $\widehat{P}_f$ incorporating the uncertain model parameters $\boldsymbol{\Theta}$ can be defined as

$$\widehat{P}_f = P(h(\boldsymbol{X},\boldsymbol{\Theta}) < 0) = \int_{h(\boldsymbol{X},\boldsymbol{\Theta})<0}\int p_X(\boldsymbol{x}|\boldsymbol{\Theta})p(\boldsymbol{\Theta}|D)\mathrm{d}\boldsymbol{\Theta}\mathrm{d}\boldsymbol{x} \tag{41}$$

where $p_X(\boldsymbol{x}|\boldsymbol{\Theta})$ is the joint PDF of $\boldsymbol{X} = \{R,S\}$; and $p(\boldsymbol{\Theta}|\boldsymbol{D})$ is the posterior PDF of $\boldsymbol{\Theta}$ conditional on monitoring/test data $\boldsymbol{D}$. If the posterior PDF $p(\boldsymbol{\Theta}|\boldsymbol{D})$ is obtained by an MCMC algorithm, $\widehat{P}_f$ can be efficiently estimated using the posterior samples $\boldsymbol{\Theta}^{(g)}(g = 1,\cdots,G)$:

$$\widehat{P}_f = G^{-1}\sum_{g=1}^{G} P_f(\boldsymbol{\Theta}^{(g)}) = G^{-1}\sum_{g=1}^{G}\int_{h(\boldsymbol{X},\boldsymbol{\Theta}^{(g)})\langle 0} p_X(\boldsymbol{x}|\boldsymbol{\Theta}^{(g)})\mathrm{d}\boldsymbol{x} \tag{42}$$

where $P_f(\boldsymbol{\Theta})$ is the conditional failure probability given the posterior samples of $\boldsymbol{\Theta}$. The existing computational tools for reliability analysis, such as the first-order reliability method (FORM), the second-order reliability method (SORM), and importance sampling (IS) method, can be applied to obtain the samples of $P_f(\boldsymbol{\Theta})$ [45].

The resistance R and load effect S can be viewed as mutually independent random variables, i.e., $p_X(\boldsymbol{x}|\boldsymbol{\Theta}) = p_R(r|\boldsymbol{\theta}_R)p_S(s|\boldsymbol{\theta}_S)$. In general, R can be properly expressed by a unimodal distribution model. In the present study, S is represented by the parametric Bayesian mixture model that is elicited from SHM data. In accordance with the posterior samples from Gibbs sampler, the samples of $P_f(\boldsymbol{\Theta})$ can be obtained as

$$\begin{aligned} P_f(\boldsymbol{\Theta}^{(g)}) &= \int_{h(\boldsymbol{X},\boldsymbol{\Theta}^{(g)})\langle 0} p_R\left(r\middle|\boldsymbol{\theta}_R^{(g)}\right)\left(\sum_{k=1}^{K}\omega_{S_k}^{(g)}p_{S_k}\left(s\middle|\boldsymbol{\theta}_{S_k}^{(g)}\right)\right)\mathrm{d}r\mathrm{d}s \\ &= \sum_{k=1}^{K}\omega_{S_k}^{(g)}\int_{h_k(\boldsymbol{X},\boldsymbol{\Theta}^{(g)})\langle 0} p_R\left(r\middle|\boldsymbol{\theta}_R^{(g)}\right)p_{S_k}\left(s\middle|\boldsymbol{\theta}_{S_k}^{(g)}\right)\mathrm{d}r\mathrm{d}s \end{aligned} \tag{43}$$

where S_k denotes the kth component of the multi-load effect; $p_{S_k}(s|\boldsymbol{\theta}_{S_k})$ and ω_{S_k} are the component density and the mixing weight associated with the kth component, respectively; and $\bigcup_{k=1}^{K} h_k(\boldsymbol{X},\boldsymbol{\Theta}) = h(\boldsymbol{X},\boldsymbol{\Theta})$ is the failure domain conditional on $\boldsymbol{\Theta}$. When R and S_k conform to the Gaussian distribution, Eq. (43) can be estimated by the FORM as

$$P_f(\Theta^{(g)}) \approx \sum_{k=1}^{K}\omega_{S_k}^{(g)}\Phi\left(-\beta_k\left(\boldsymbol{\theta}_R^{(g)},\boldsymbol{\theta}_{S_k}^{(g)}\right)\right) \tag{44}$$

where $\beta_k(\boldsymbol{\theta}_R,\boldsymbol{\theta}_{S_k}) = (\mu_R - \mu_{S_k})/\left(\sigma_R^2 + \sigma_{S_k}^2\right)^{1/2}$ is the reliability estimate associated with the kth component of load effect conditional on $\boldsymbol{\theta}_R$ and $\boldsymbol{\theta}_{S_k}$. It follows immediately that the samples of $\beta(\boldsymbol{\Theta})$, termed as the estimate of conditional reliability index, are obtained as

$$\beta(\boldsymbol{\Theta}^{(g)}) = -\Phi^{-1}(P_f(\boldsymbol{\Theta}^{(g)})) = -\Phi^{-1}\left(\sum_{k=1}^{K}\omega_{S_k}^{(g)}\Phi\left(-\frac{\mu_R - \mu_{S_k}^{(g)}}{\sqrt{\sigma_R^2 + \sigma_{S_k}^{2(g)}}}\right)\right) \tag{45}$$

where Φ^{-1} is the inverse cumulative probability density of the standard normal distribution; $\omega_{S_k}^{(g)}$, $\mu_{S_k}^{(g)}$ and $\sigma_{S_k}^{2(g)}$ $(g = 1,\cdots,G)$ are posterior samples of the mixture parameters from the Gibbs iteration. Eq. (45) provides a general expression to calculate the conditional reliability index in terms of the FGM model. It unveils that the sample value of the conditional reliability index $\beta(\boldsymbol{\Theta})$ is a function with respect to the uncertain model parameters $\boldsymbol{\Theta}$, leading $\beta(\boldsymbol{\Theta})$ itself to be a random variable due to the nature of uncertainty of $\boldsymbol{\Theta}$. In this sense, not only the intrinsic variability of the resistance and load effect, but also the uncertainty arising from parametric modelling and measurement error, have influence on the reliability assessment. The reliability index estimate $\widehat{\beta}$ considering both aleatory uncertainty and epistemic uncertainty can thus be determined as the sample mean of $\beta(\boldsymbol{\Theta})$:

$$\widehat{\beta} = \mu_\beta = G^{-1}\sum_{g=1}^{G}\beta(\Theta^{(g)}) \tag{46}$$

and the sample standard deviation of $\beta(\boldsymbol{\Theta})$ quantifies the variation in the reliability index estimate induced by various uncertainties:

$$\sigma_\beta = \sqrt{(G-1)^{-1}\sum_{g=1}^{G}(\beta(\boldsymbol{\Theta}^{(g)}) - \mu_\beta)^2} \tag{47}$$

3.2. Successive updating of reliability index

With successively collected SHM data, the conditional reliability index β (the symbol $\boldsymbol{\Theta}$ is omitted hereafter for brevity) can be updated at regular intervals in order to evolutionarily assess the structural condition. Assume that β conforms to the Gaussian distribution with uncertain parameters $\theta_\beta = \{\mu_\beta,\sigma_\beta^2\}$, and suppose the samples of $\beta^m \sim \mathcal{N}(\beta|\theta_\beta^m)$ in relation to the mth monitoring period have been obtained using Eq. (45) with the monitoring data D^m. When newly collected monitoring data D^{m+1} become available, the samples of β^{m+1} in relation to the $(m+1)$th monitoring period can be obtained by following the same manner. It is apparent that β^{m+1} estimated solely using the dataset D^{m+1} is inadequate to portray the current structural condition, but rather it should be combined with the historical knowledge of the earlier reliability estimate β^m. By applying Bayes' theorem, the following formula can be reached to seek the posterior distribution of θ_β^{m+1}:

$$p(\theta_\beta^{m+1}|\beta^{m+1}) \propto p(\beta^{m+1}|\theta_\beta^m)p(\theta_\beta^m) \tag{48}$$

where $p(\theta_\beta^m)$ is the posterior distribution of θ_β for the mth monitoring period and it is also the prior distribution of θ_β for the $(m+1)$th monitoring period. The successive reliability index updating of β is achieved by repeatedly evaluating the posterior predictive distribution:

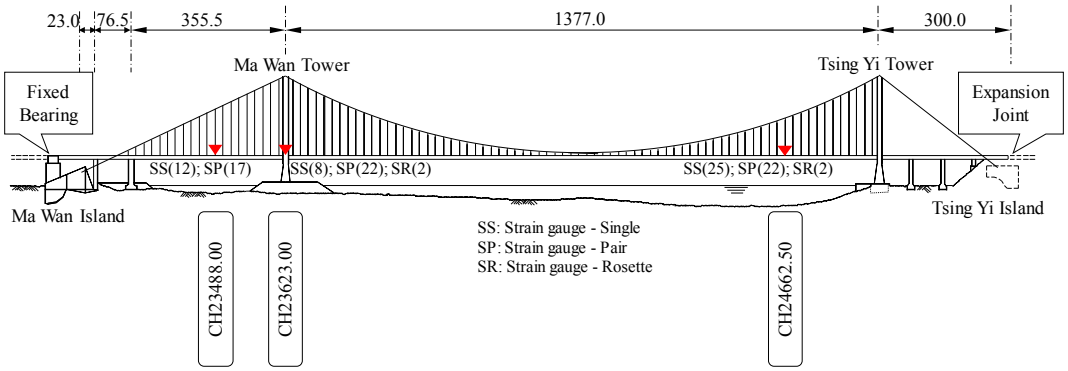

Fig. 3. TMB and sections instrumented with strain sensors.

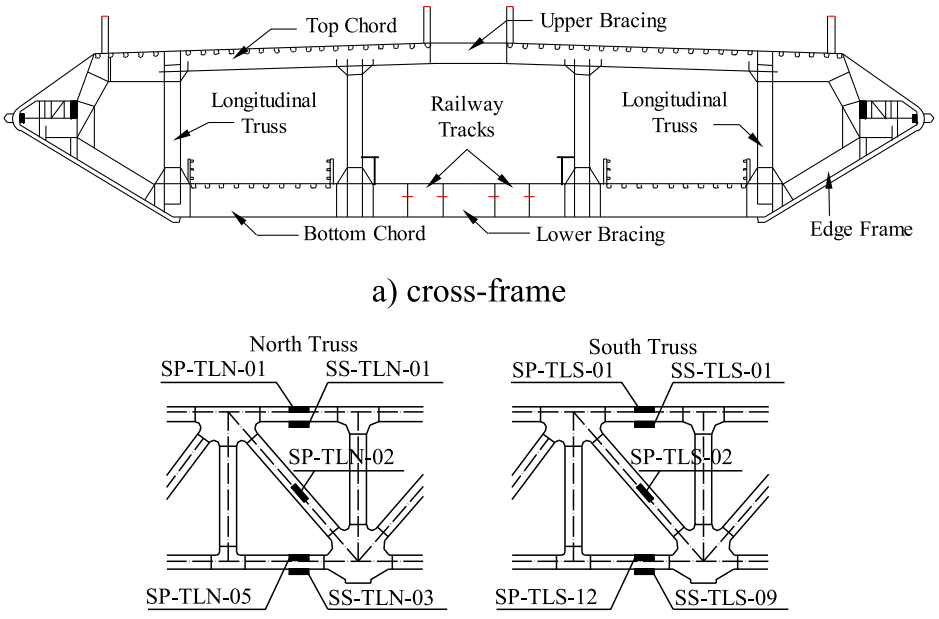

Fig. 4. Deck cross-frame and longitudinal truss of TMB.

$$p(\tilde{\beta}^{m+1}|\beta^{m+1}) = \int p(\tilde{\beta}^{m+1}|\theta_{\beta}^{m+1},\beta^{m+1})p(\theta_{\beta}^{m+1}|\beta^{m+1})\mathrm{d}\theta_{\beta}^{m+1} \tag{49}$$

where $\tilde{\beta}^{m+1}$ is the predictive reliability index in relation to the $(m+1)$th monitoring period. Apparently, $\tilde{\beta}^{m+1}$ is more informative than β^{m+1} in evaluating the structural condition in that the former incorporates the previously inferred structural condition knowledge. When the monitoring data are cumulatively available, the Bayesian updating scheme enables to generate the condition assessment results evolutionarily over the entire monitoring period. Note that Eq. (49) can be solved analytically if the conjugate prior of θ_{β} is employed [26].

4. Application to instrumented Tsing Ma bridge

4.1. Tsing Ma bridge and its instrumentation

The Tsing Ma Bridge (TMB) as illustrated in Fig. 3 is a suspension bridge with a main span of 1377 m in Hong Kong, carrying both highway and railway traffic between the airport and city center. With awareness of the importance of the bridge, a sophisticated long-term SHM system has been instrumented on the TMB by the Hong Kong SAR Government Highways Department. Apart from other categories of sensors, a total of 110 strain gauges were installed at three bridge deck sections denoted by CH23488.00, CH23623.00 and CH24662.50 in Fig. 3, providing continuous dynamic strain measurements. Fig. 4 shows a typical deck cross-section as well as two instrumented longitudinal trusses where three types of strain gauges (single, pair and rosette) are deployed on the truss elements (top chords, diagonal struts and bottom chords). The sampling rate for strain data acquisition was set to 51.2 Hz. In-service monitoring captures authentic strain responses experienced by the bridge under operational condition, which can help track the safety reserve of structural components and provide information regarding the load-carry capacity of the whole bridge.

One-year continuous monitoring data of strain under the routine operation of the TMB are collected for this study. Fig. 5(a) shows the raw strain sequence in one day measured by sensor SP-TLN-01 deployed at the top chord of the north longitudinal truss at Section CH24662.50, where positive value denotes compressive strain and negative value denotes tension strain. The measured strain is mainly generated by highway traffic, railway traffic, wind, and temperature. The static strain due to initial dead loads is not measurable because the sensors were installed after the completion of bridge construction. It is observed from Fig. 5(a) that the strain between 2:00 and 5:00 am is obviously small

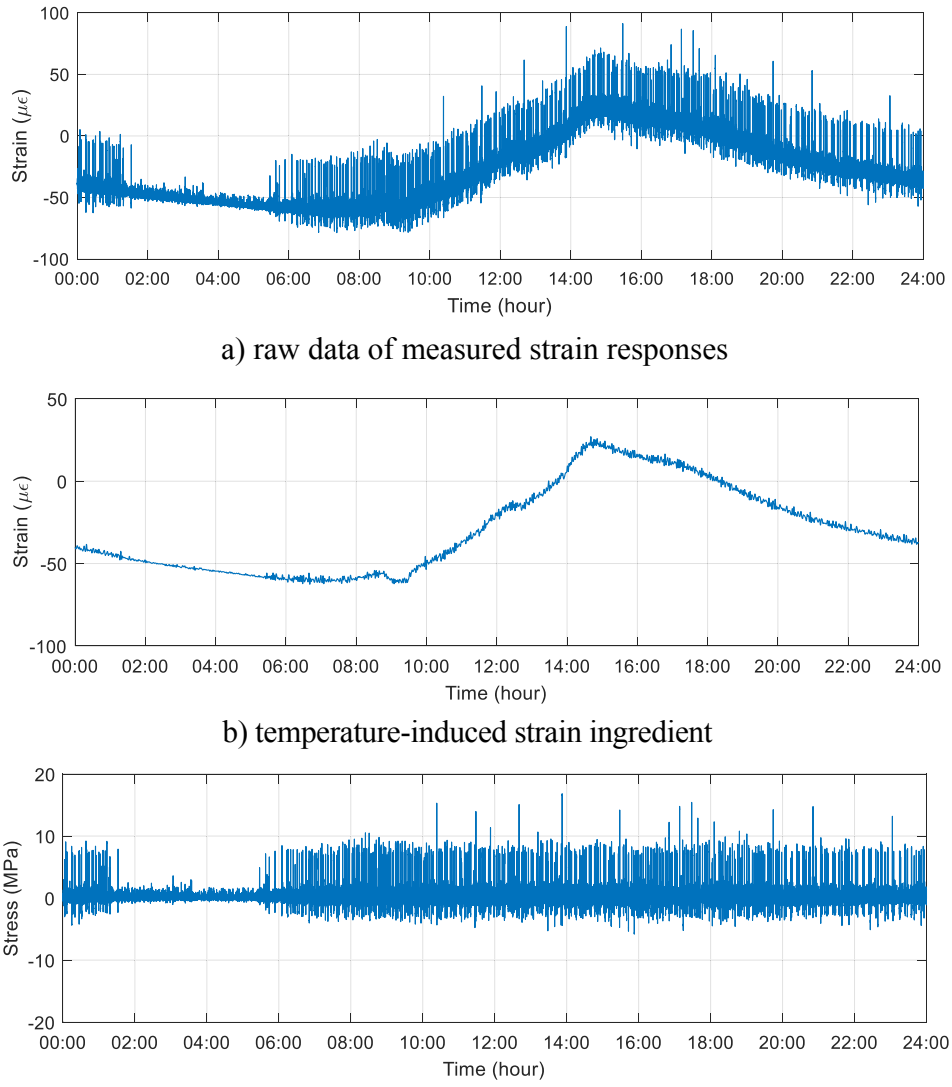

Fig. 5. 24-hour strain time history at top chord.

since the railway traffic ceased to operate during that period. It is also found that there is a trend ingredient in the strain sequence over 24-hour time period, which has been demonstrated to be the effect of daily temperature variation [17]. The temperature-induced strain, although quite large, contributes little to the stress because the majority of it is released by free movement of the bridge deck at the expansion joints. Hence, in subsequent reliability analysis, the temperature-induced strain as absorbed by the expansion joint is excluded from the total strain. A wavelet-based multi-component decomposition procedure [17] has been developed to separate the temperature-induced strain as depicted in Fig. 5(b), and the strain sequence after eliminating the temperature effect is illustrated in Fig. 5(c). Discrete Wavelet Transform (DWT) enables a signal to be decomposed into various resolution scales: the decomposed ones with coarse resolution (approximations) contain the information about low-frequency components, and the decomposed ones with fine resolution (details) contain the information about high-frequency components. Making use of the wavelet-level selection and perfect reconstruction (PR) properties of DWT for multi-resolution analysis, the strain ingredient caused by daily temperature variation can be extracted from the raw measurement data.

The live load-induced stress responses are then obtained by multiplying the strains by the elastic modulus E of steel in view of the fact that the bridge is in elastic state under normal operational environment. Fig. 6 shows the monitoring-derived stress sequences in 30 min under live loads for the top chord, diagonal strut and bottom chord of the north longitudinal truss at Section CH24662.50. From the stress time histories, peak stress points are extracted by using an adaptive peak counting method [55] to construct the peak stress sequences as shown in Fig. 7. It is observed that the peak stress values are randomly dispersed but mostly clustered to two stress levels of different amplitudes. The peak values around the higher amplitude level are recognized as railway-induced stress responses, while the peak values around the lower amplitude level are mainly caused by highway traffic. The action of wind loading is a non-stationary process, and its effect under normal wind conditions in general causes the in-between values among the two levels. The peak stress values above the higher amplitude level are primarily stemming from two scenarios: (i) two trains passing each other in opposite directions on the bridge (approximately two such events occur in one hour) and (ii) strong winds (e.g. typhoons) hitting the bridge in combination with highway/railway traffic. The histograms of the peak stresses are obtained as shown in Fig. 8. It is obviously observed that all the stress distributions exhibit multimodal response feature.

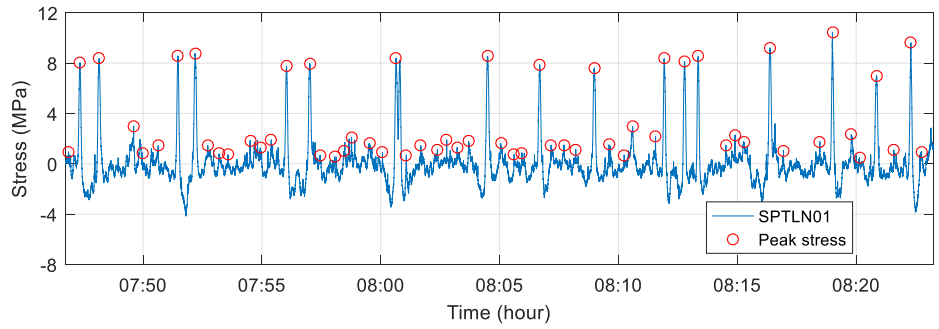

a) top chord

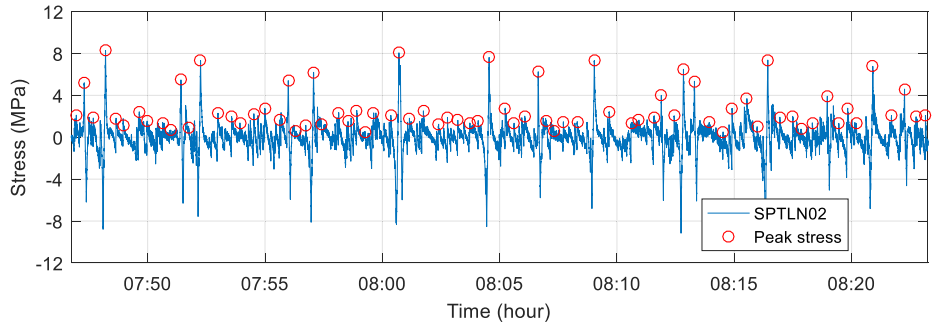

b) diagonal strut

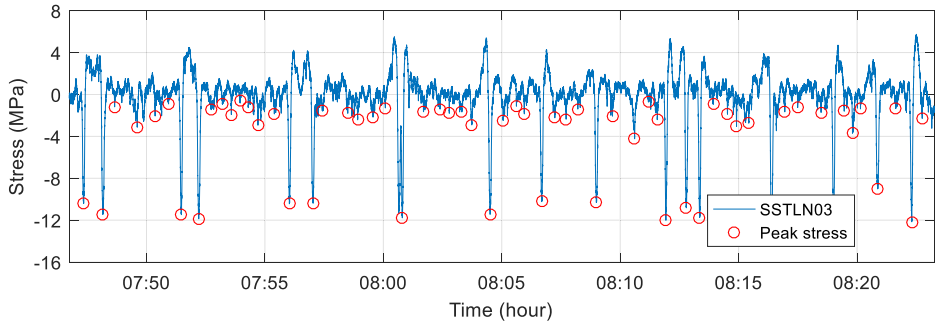

c) bottom chord

Fig. 6. Stress responses and identified peak stresses in 30-minute temporal scale.

4.2. Formulation of parametric Bayesian mixture models

The parametric Bayesian mixture modelling procedure presented in Section 2, including the Gibbs sampler and Bayes factor-based model order selection, is applied to the peak stress sequences for the estimation of uncertain model parameters and quantification of uncertainties. For illustration purpose, the stress responses of top chord in January are taken as an example. At the stage of parameter estimation, the Gibbs sampler is set to run for $T = 10000$ iterations. Fig. 9 plots the Gibbs iterations for each mixture parameter. It is seen that the Markov chains quickly reach stationary after only few dispersed samples coming from the early draws. To quantitatively examine the convergence of the Markov chains, the scale reduction factor R_0 of each mixture parameter is monitored through the Gibbs run as illustrated in Fig. 10. As the iteration continues, the values of R_0 for all parameters quickly decline to 1, indicating the iterations converge globally. From the convergence statistics listed in Table 1, it is found that the variances (σ^2) reach convergence fastest, following by the mixing weights (ω), while the stabilization of the means (μ) is the slowest in this case. Based on the convergence results, the number of burn-in samples of the Gibbs iterations is determined as $B = 5000$. Then the rest of $G = T - B = 5000$ Gibbs outputs are deemed as stationary posterior samples of the target distributions, which are then used for parameter estimation.

Table 2 lists the identified number of mixture components and the estimated parameters (including mean value and 95% confidence interval) of the posterior FGM models for multimodal load effects of the top chord, diagonal strut and bottom chord. To verify the efficacy of the proposed Bayesian approach, the parameter estimation obtained by the conventional frequentist approach using expectation maximization algorithm [22] is also provided in Table 2. It is seen that the mean values elicited from the Bayesian approach are close to the point estimates of the frequentist approach. Given the posterior FGM models, the predictive PDFs and associated 5–95 uncertain bounds are constructed as depicted in Fig. 11. The predictive PDFs fit well with the histograms of multimodal stress responses for all the three truss members. The upper and lower uncertain bounds unveil the variability in PDF estimation of the FGM models due to parametric uncertainty. By comparing the Bayes factor (logarithm of the marginal likelihood) of each candidate model as illustrated in Fig. 12, the optimal model order (number of mixture components) is identified to be 4 for the top and bottom chords and 3 for

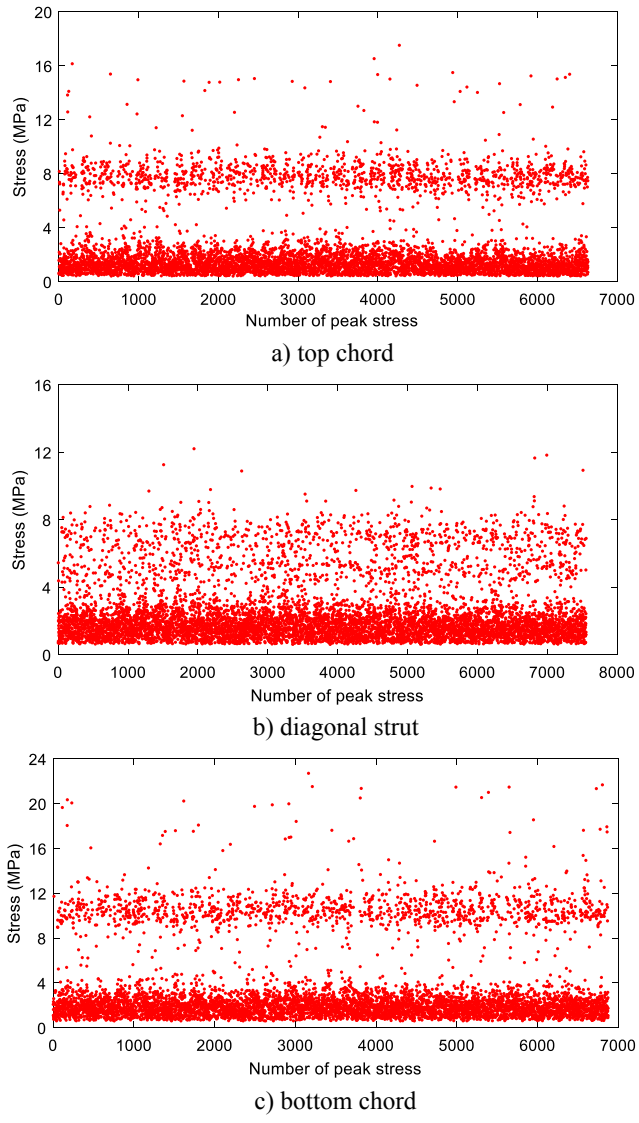

Fig. 7. Extracted peak stresses in one-month temporal scale.

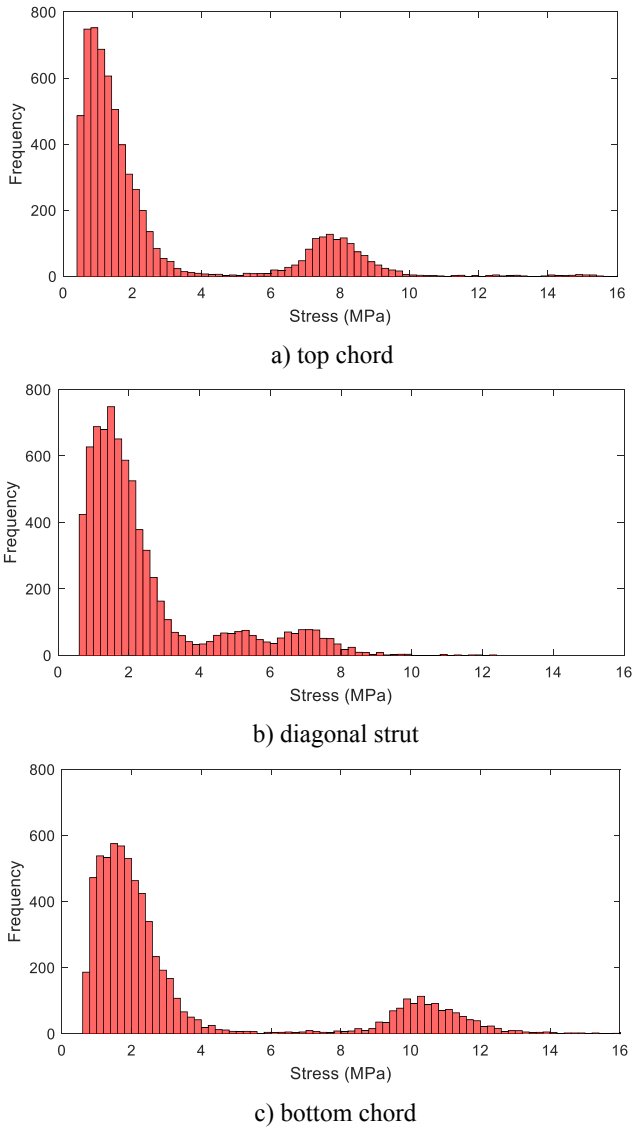

Fig. 8. Histograms of peak stresses derived from one-month data.

the diagonal strut. Although four mixture components are needed for the top and bottom chords, the weight (ω_k) of the fourth component is much less than those of the first three components while the variance (σ_k^2) of the fourth component is much larger than the first three. It is worth mentioning that extreme load effects due to heavy-duty railway traffic, gust wind during strong typhoons, and their combination, as compared with regular loading, are far more indeterminate, causing sparse and dispersed values in the tail region, which may have an marked influence on the reliability assessment. The mixture models equipped with sufficient components enable to capture the tail characteristics reasonably and thus facilitate a high-fidelity estimate of reliability index.

4.3. Successive assessment of reliability index

According to the design documents of the TMB, the maximum allowable stress for the truss members under live loads in serviceability limit state is specified as 60 MPa [56]. The coefficient of variation is taken as $\gamma = 0.075$ [11,57]. These statistics serve as the probability descriptors of resistance R, which yield a mean value $\mu_R = 60$ MPa and a standard deviation (std) $\sigma_R = \gamma\mu_R = 4.5$ MPa for assessment (since no durability-relevant sensors were installed on the TMB, we are unable to formulate the distribution and deterioration models of resistance from SHM data). With the load effect (stress) formulated in terms of parametric Bayesian mixture models, the samples of conditional reliability index can be readily evaluated using Eq. (45). Fig. 13 provides the obtained conditional reliability indices (in the form of probability distributions) in regard to the Bayesian mixture models formulated using one-month data (as shown in Table 2 and Fig. 11) for the top chord, diagonal strut and bottom chord. It is seen that the diagonal strut has the highest reliability index (mean = 11.482, std = 0.032), the top chord comes to the second (mean = 9.089, std = 0.218), and the bottom chord stands to have the lowest reliability index (mean = 7.882, std = 0.207). In addition, the reliability index for the diagonal strut has much less uncertainty than the top and bottom chords. For comparison, the reliability indices obtained from the conventional frequentist approach using the same data set are also provided in Table 3. It is found that the mean values of the conditional reliability indices obtained by the Bayesian approach are in favorable agreement with those obtained by the conventional frequentist approach.

The conditional reliability index can be gradually updated with successively collected SHM data. It is illustrated in Figs. 14 and 15. In Fig. 14(a), the blue curve denotes the conditional reliability index of the top chord obtained using SHM data collected in the first month (January), same as shown in Fig. 13. When SHM data in the second month (February) are obtained as depicted by the gray curve, the

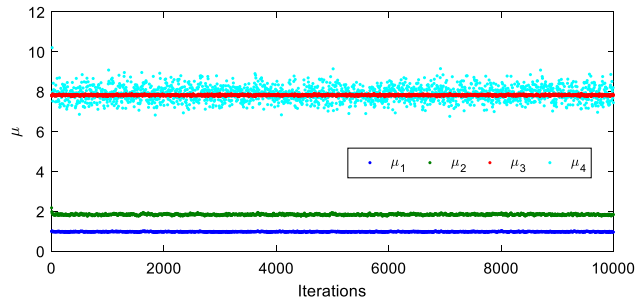

a) Gibbs iterations for μ

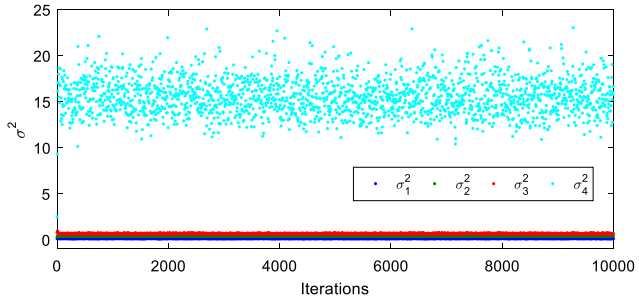

b) Gibbs iterations for σ^2

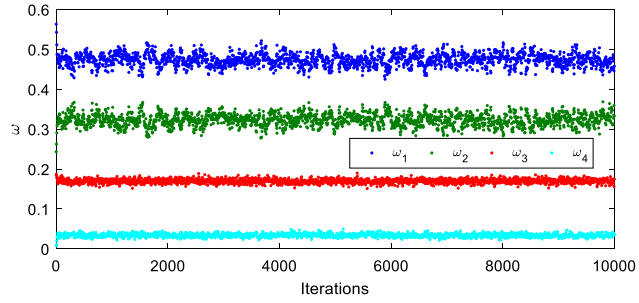

c) Gibbs iterations for ω

Fig. 9. Gibbs iterations for mixture parameters.

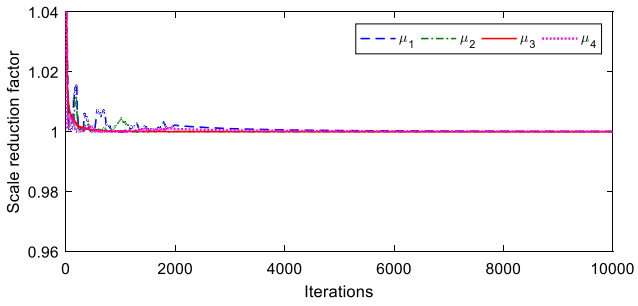

a) scale reduction factor for μ

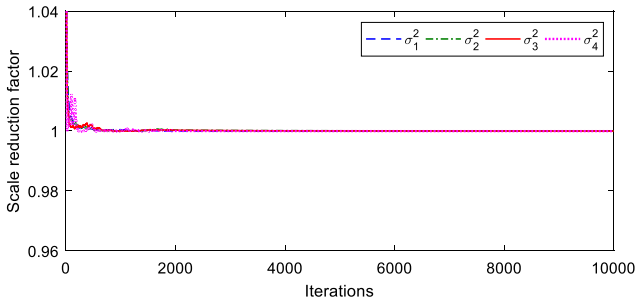

b) scale reduction factor for σ^2

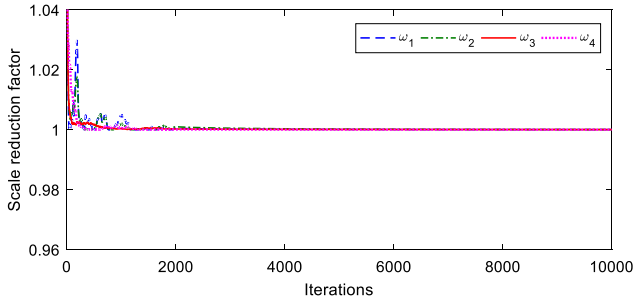

c) scale reduction factor for ω

Fig. 10. Convergence evaluation based on scale reduction factor.

conditional reliability index is updated by combining the previously obtained conditional reliability index (as prior distribution) and the newly collected monitoring data (as likelihood), with the updated result shown by the red curve. The conjugate priors adopted greatly facilitate the Bayesian updating of conditional reliability index. Because one-year monitoring data are available for the case study, the conditional reliability index can be gradually updated month-by-month as shown in Fig. 15(a) if SHM data acquired in one month are used to formulate Bayesian mixture models each time. Similarly, reliability updating results of the diagonal strut are depicted in Fig. 14(b) and Fig. 15(b), and those of the bottom chord are given in Fig. 14(c) and Fig. 15(c).

Fig. 16 illustrates the evolution of the means and standard deviations of the predictive reliability indices for the top chord, diagonal strut and bottom chord in one year. It is seen that the predictive reliability index for the diagonal strut approaches to be stationary very soon with small standard deviation. The predictive reliability indices for the top and bottom chords reach stationarity after updating with SHM data acquired in about six months. After being stationary, the standard deviations of the predictive reliability indices for the top chord and bottom chord are nearly identical, but the mean values are different. It is observed that the predictive reliability indices obtained for the top chord and bottom chord in March significantly deviate from those in other months. This is due to the insufficient SHM data collected in March because the data acquisition station was malfunctioning for days in that month, as evidenced by Fig. 17. It concludes that the data (sample) size is influential to the estimate of conditional reliability index. According to the relationship between reliability index and maintenance action [58], it is judged that the diagonal strut ($\beta > 11$) is in excellent condition with no need of inspection; the top chord ($\beta > 8$ with its mean around 9) is in good condition just needing preventive inspection; and the bottom chord ($\beta > 6$ with its mean less than 8) is in satisfactory condition but needs regular inspection. In addition to the mean value, the standard deviation of the conditional reliability index is also helpful in risk assessment when the bridge owner schedules bridge inspection and maintenance strategy.

Table 1
Convergence statistics for Gibbs sampler.

Component	Parameterμ	Parameterσ^2	Parameterω
	Gibbs iterations needed to reach convergence ($R_0 < 1.001$)		
No. 1	2982	453	1798
No. 2	1160	392	1815
No. 3	378	614	617
No. 4	1937	491	1113

Table 2
Modelling of multimodal stress responses.

Component	Parameterμ				Parameterσ^2				Parameterω			
	Bayesian estimation			Frequentist estimation	Bayesian estimation			Frequentist estimation	Bayesian estimation			Frequentist estimation
	5%	Mean	95%		5%	Mean	95%		5%	Mean	95%	
Top chord												
No. 1	0.952	**0.972**	0.992	0.871	0.110	**0.119**	0.128	0.066	0.449	**0.474**	0.499	0.370
No. 2	1.784	**1.832**	1.882	1.694	0.357	**0.387**	0.419	0.330	0.299	**0.323**	0.347	0.423
No. 3	7.775	**7.820**	7.865	7.835	0.602	**0.663**	0.728	0.539	0.161	**0.170**	0.178	0.162
No. 4	7.285	**7.896**	8.519	7.378	12.730	**15.595**	19.016	13.827	0.027	**0.034**	0.041	0.045
Diagonal strut												
No. 1	1.145	**1.174**	1.204	1.074	0.097	**0.108**	0.120	0.065	0.319	**0.350**	0.382	0.262
No. 2	1.971	**2.014**	2.060	1.916	0.300	**0.324**	0.348	0.310	0.427	**0.460**	0.490	0.542
No. 3	5.661	**5.771**	5.877	5.694	2.393	**2.631**	2.894	2.766	0.182	**0.191**	0.199	0.196
Bottom chord												
No. 1	1.493	**1.539**	1.585	1.297	0.246	**0.272**	0.301	0.128	0.476	**0.523**	0.570	0.327
No. 2	2.399	**2.492**	2.596	2.242	0.588	**0.651**	0.720	0.484	0.234	**0.280**	0.326	0.471
No. 3	10.424	**10.480**	10.537	10.488	0.886	**0.981**	1.083	0.766	0.149	**0.157**	0.166	0.150
No. 4	9.757	**10.396**	11.058	9.725	19.872	**24.008**	28.773	22.328	0.033	**0.039**	0.046	0.051

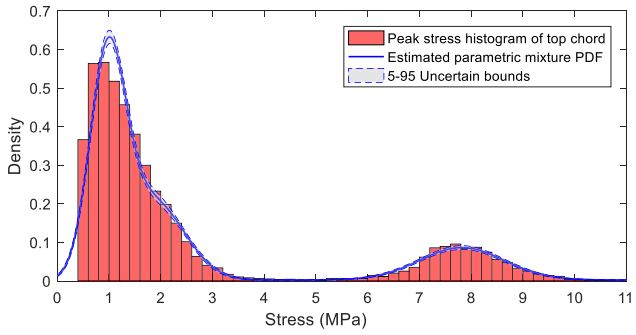

a) top chord

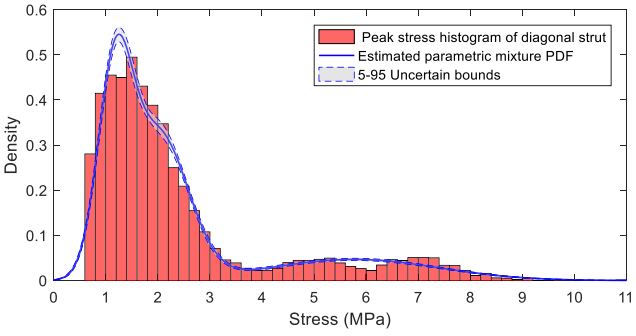

b) diagonal struct

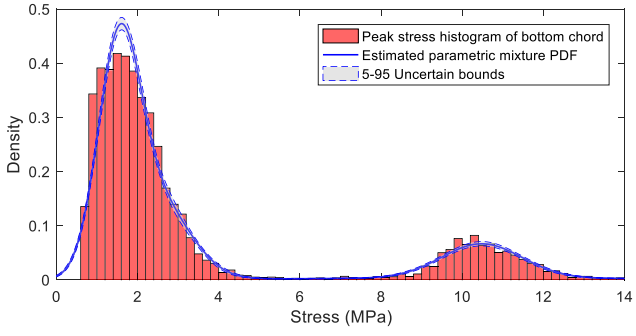

c) bottom chord

Fig. 11. Estimated mixture PDF of stress response with uncertain bounds.

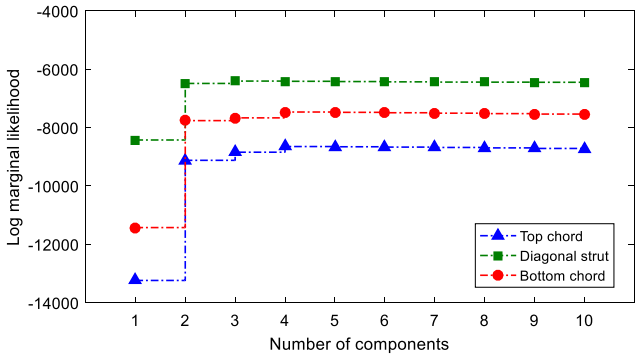

Fig. 12. Optimal model order based on Bayes factor.

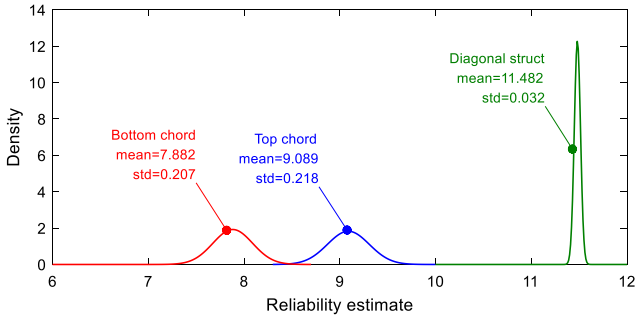

Fig. 13. Conditional reliability indices based on one-month monitoring data.

Table 3
Comparison of Bayesian approach and frequentist approach on reliability estimate.

	Reliability estimate		
	Top chord	Diagonal strut	Bottom chord
Bayesian FGM model	9.089	11.482	7.882
Conventional FGM model	9.349	11.462	8.075

5. Conclusions

A monitoring-based bridge component reliability assessment method in terms of parametric Bayesian mixture modelling was developed in this study. In contrast with the conventional frequentist approach, the Bayesian treatment enriches the mixture model by providing not only

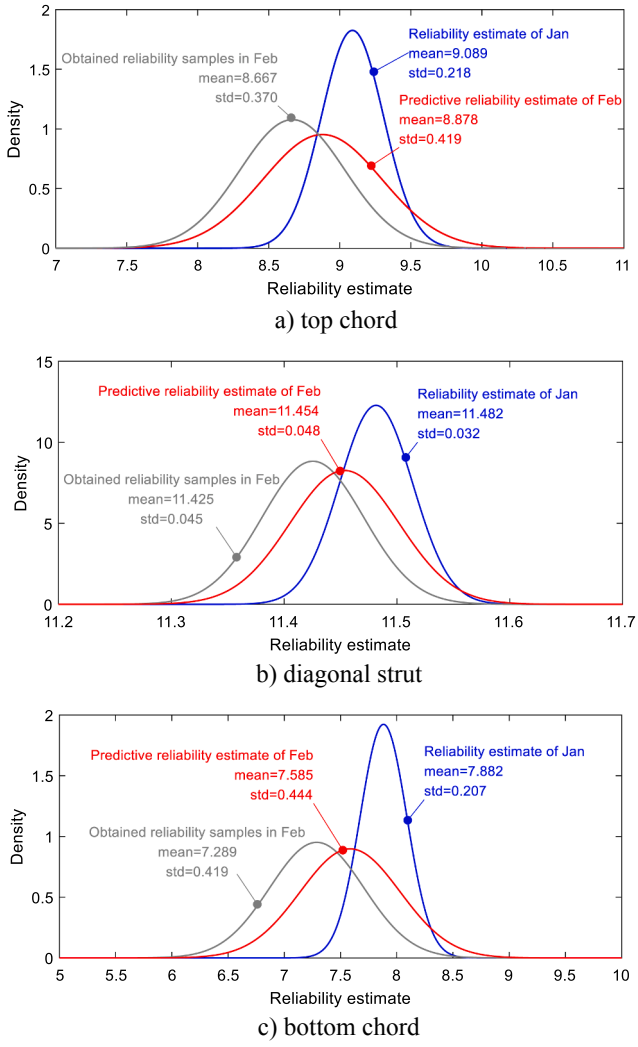

Fig. 14. One-month reliability updating for top chord, diagonal strut and bottom chord.

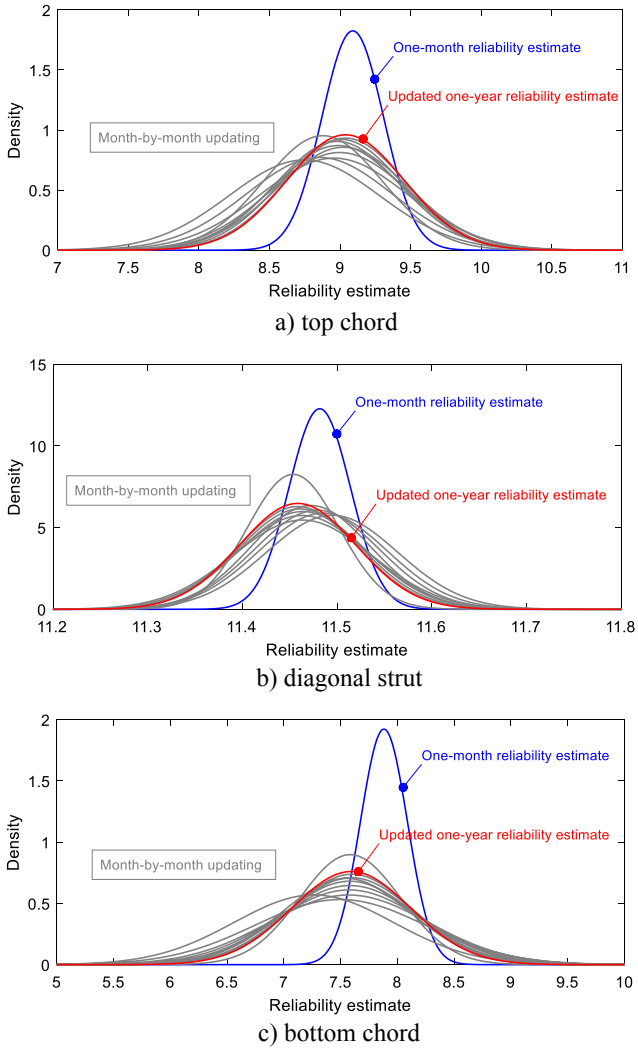

Fig. 15. One-year reliability updating for top chord, diagonal strut and bottom chord.

most plausible parameter estimates but also the associated uncertainty levels. In this connection, the formulated Bayesian mixture model is capable of accommodating multimodal structural responses while considering parametric uncertainty; the estimated conditional reliability index allows accounting for both aleatory and epistemic uncertainties arising from resistance and load effect characterization and can be successively updated with the accumulation of monitoring data. Because of the presence of various uncertainties and incompleteness of the monitoring data, the estimated conditional reliability index is no longer a fixed value but rather a random variable that is affected by uncertainties arising from resistance and load effect, inclusive of the measurement error, uncertain model parameters, as well as incompleteness and heterogeneity of the monitoring data. The Bayesian paradigm offers an adequate avenue to incorporate prior knowledge retained in the previous data into the estimate of reliability index using the current data.

The feasibility of the proposed method is demonstrated by using one-year strain monitoring data collected by an SHM system deployed on the suspension Tsing Ma Bridge (TMB). The case study comes to the following points: (i) the parametric Bayesian mixture models embracing a few component densities can favorably characterize the heterogeneous stress responses with multimodality, resulting from the combined action of multiple live loads such as highway traffic, railway traffic, monsoons and typhoons; (ii) in the situation of having only insufficient monitoring

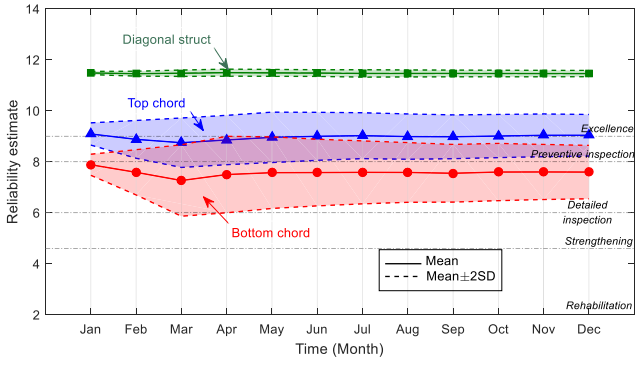

Fig. 16. Evolution of predictive reliability indices over time.

data, the estimated results of the conditional reliability index may be noticeably biased, but more persuasive results can be achieved with the accumulation of monitoring data; (iii) stationary estimates of the conditional reliability index can be reached after successive updating with sufficient monitoring data lasting for several months; and (iv) the estimated reliability indices (including means and standard deviations) from different structural members can be linked up to scheduling and

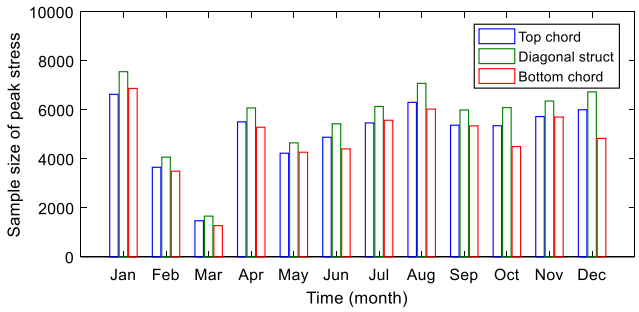

Fig. 17. Size of peak stress samples used for successive reliability assessment.

prioritizing bridge inspection and maintenance activities in compliance with a certain risk threshold.

CRediT authorship contribution statement

Y.Q. Ni: Conceptualization, Methodology, Validation, Resources, Writing - review & editing, Supervision, Project administration, Funding acquisition. **R. Chen:** Data curation, Software, Formal analysis, Investigation, Writing - original draft, Visualization.

Declaration of Competing Interest

The authors declare that they have no known competing financial interests or personal relationships that could have appeared to influence the work reported in this paper.

Acknowledgements

The work described was supported by a grant from the Research Grants Council of the Hong Kong Special Administrative (SAR) Region, China (Grant No. PolyU 152241/15E) and a grant from the National Natural Science Foundation of China (Grant No. U1934209). The authors would also like to appreciate the funding support by the Innovation and Technology Commission of the Hong Kong SAR Government (Grant No. K-BBY1).

Appendix A. Supplementary material

Supplementary data to this article can be found online at https://doi.org/10.1016/j.engstruct.2020.111406.

References

[1] Catbas FN, Aktan AE. Condition and damage assessment: issues and some promising indices. J Struct Eng (ASCE) 2002;128(8):1026–36.
[2] Mufti AA. Structural health monitoring of innovative Canadian civil engineering structures. Struct Health Monitor 2002;1(1):89–103.
[3] Ko JM, Ni YQ. Technology developments in structural health monitoring of large-scale bridges. Eng Struct 2005;27(12):1715–25.
[4] Brownjohn JMW. Structural health monitoring of civil infrastructure. Philo Trans Royal Soc A Math Phys Eng Sciences 1851;2007(365):589–622.
[5] Ou JP, Li H. Structural health monitoring in mainland China: review and future trends. Struct Health Monitor 2010;9(3):219–31.
[6] Fujino Y, Siringoringo DM. Bridge monitoring in Japan: the needs and strategies. Struct Infrastruct Eng 2011;7(7–8):597–611.
[7] Ni YQ, Wong KY, Xia Y. Health checks through landmark bridges to sky-high structures. Adv Struct Eng 2011;14(1):103–19.
[8] Nguyen A, Chan THT, Zhu X. Real world application of SHM in Australia. Struct Health Monitor 2019;18(1):3–4.
[9] Ni YQ, Hua XG, Ko JM. Reliability-based assessment of bridges using long-term monitoring data. Key Eng Mater 2006;321–323:217–22.
[10] Catbas FN, Susoy M, Frangopol DM. Structural health monitoring and reliability estimation: Long span truss bridge application with environmental monitoring data. Eng Struct 2008;30(6):2347–59.
[11] Frangopol DM, Strauss A, Kim S. Bridge reliability assessment based on monitoring. J Bridge Eng (ASCE) 2008;13(3):258–70.
[12] Hosser D, Klinzmann C, Schnetgöke R. A framework for reliability-based system assessment based on structural health monitoring. Struct Infrastruct Eng 2008;4(4):271–85.
[13] Liu M, Frangopol DM, Kim S. Bridge safety evaluation based on monitored live load effects. J Bridge Eng (ASCE) 2009;14(4):257–69.
[14] Messervey TB, Frangopol DM, Casciati S. Application of the statistics of extremes to the reliability assessment and performance prediction of monitored highway bridges. Struct Infrastruct Eng 2011;7(1–2):87–99.
[15] Ni YQ, Ye XW, Ko JM. Monitoring-based fatigue reliability assessment of steel bridges: analytical model and application. J Struct Eng (ASCE) 2010;136(12):1563–73.
[16] Li H, Li SL, Ou JP, Li HW. Reliability assessment of cable-stayed bridges based on structural health monitoring techniques. Struct Infrastruct Eng 2012;8(9):829–45.
[17] Ni YQ, Xia HW, Wong KY, Ko JM. In-service condition assessment of bridge deck using long-term monitoring data of strain response. J Bridge Eng (ASCE) 2012;17(6):876–85.
[18] McLachlan G, Peel D. Finite mixture models. New York, NY: John Wiley & Sons; 2000.
[19] Frühwirth-Schnatter S. Finite mixture and Markov switching models. New York, NY: Springer Science & Business Media; 2006.
[20] Nair KK, Kiremidjian AS. Time series based structural damage detection algorithm using Gaussian mixtures modeling. J Dynamic Syst Measurement Control (ASME) 2007;129(3):285–93.
[21] Ni YQ, Ye XW, Ko JM. Modeling of stress spectrum using long-term monitoring data and finite mixture distributions. J Eng Mech (ASCE) 2012;138(2):175–83.
[22] Xia HW, Ni YQ, Wong KY, Ko JM. Reliability-based condition assessment of in-service bridges using mixture distribution models. Comput Struct 2012;106–107:204–13.
[23] Enright B, OBrien EJ. Monte Carlo simulation of extreme traffic loading on short and medium span bridges. Struct Infrastruct Eng 2013;9(12):1267–82.
[24] Farhidzadeh A, Salamone S, Singla P. A probabilistic approach for damage identification and crack mode classification in reinforced concrete structures. J Intell Mater Syst Struct 2013;24(14):1722–35.
[25] Li S, Wei S, Bao Y, Li H. Condition assessment of cables by pattern recognition of vehicle-induced cable tension ratio. Eng Struct 2018;155:1–15.
[26] Gelman A, Carlin JB, Stern HS, Dunson DB, Vehtari A, Rubin DB. Bayesian data analysis (third edition). Boca Raton, FL: CRC Press; 2014.
[27] Der Kiureghian A. Bayesian analysis of model uncertainty in structural reliability. In: Der Kiureghian A, Thoft-Christensen P, editors. Reliability and Optimization of Structural Systems' 90. Berlin, Germany: Springer-Verlag; 1991. p. 211–21.
[28] Igusa T, Buonopane SG, Ellingwood BR. Bayesian analysis of uncertainty for structural engineering applications. Struct Saf 2002;24(2):165–86.
[29] Goller B, Schueller GI. Investigation of model uncertainties in Bayesian structural model updating. J Sound Vib 2011;330(25):6122–36.
[30] Beck JL, Katafygiotis LS. Updating models and their uncertainties. I: Bayesian statistical framework. J Eng Mech (ASCE) 1998;124(4):455–61.
[31] Zhang EL, Feissel P, Antoni J. A comprehensive Bayesian approach for model updating and quantification of modeling errors. Probab Eng Mech 2011;26(4):550–60.
[32] Lam HF, Peng HY, Au SK. Development of a practical algorithm for Bayesian model updating of a coupled slab system utilizing field test data. Eng Struct 2014;79:182–94.
[33] Au SK. Fast Bayesian FFT method for ambient modal identification with separated modes. J Eng Mech (ASCE) 2011;137(3):214–26.
[34] Au SK, Zhang FL, Ni YC. Bayesian operational modal analysis: theory, computation, practice. Comput Struct 2013;126:3–14.
[35] Lam HF, Yang JH, Beck JL. Bayesian operational modal analysis and assessment of a full-scale coupled structural system using the Bayes-Mode-ID method. Eng Struct 2019;186:183–202.
[36] Sohn H, Law KH. A Bayesian probabilistic approach for structure damage detection. Earthquake Eng Struct Dyn 1997;26(12):1259–81.
[37] Yuen KV, Au SK, Beck JL. Two-stage structural health monitoring approach for phase I benchmark studies. J Eng Mech (ASCE) 2004;130(1):16–33.
[38] Lam HF, Ng CT. The selection of pattern features for structural damage detection using an extended Bayesian ANN algorithm. Eng Struct 2008;30(10):2762–70.
[39] Figueiredo E, Radu L, Worden K, Farrar CR. A Bayesian approach based on a Markov-chain Monte Carlo method for damage detection under unknown sources of variability. Eng Struct 2014;80:1–10.
[40] Yin T, Jiang QH, Yuen KV. Vibration-based damage detection for structural connections using incomplete modal data by Bayesian approach and model reduction technique. Eng Struct 2017;132:260–77.
[41] Zhang RX, Mahadevan S. Model uncertainty and Bayesian updating in reliability-based inspection. Struct Saf 2000;22(2):145–60.
[42] Garbatov Y, Soares CG. Bayesian updating in the reliability assessment of maintained floating structures. J Offshore Mech Arct Eng 2002;124(3):139–45.
[43] Papadimitriou C, Beck JL, Katafygiotis LS. Updating robust reliability using structural test data. Probab Eng Mech 2001;16(2):103–13.
[44] Beck JL, Au SK. Bayesian updating of structural models and reliability using Markov chain Monte Carlo simulation. J Eng Mech (ASCE) 2002;128(4):380–91.
[45] Der Kiureghian A. Analysis of structural reliability under parameter uncertainties. Probab Eng Mech 2008;23(4):351–8.
[46] Strauss A, Frangopol DM, Kim S. Use of monitoring extreme data for the performance prediction of structures: Bayesian updating. Eng Struct 2008;30(12):3654–66.

[47] Ching J, Leu SS. Bayesian updating of reliability of civil infrastructure facilities based on condition-state data and fault-tree model. Reliab Eng Syst Saf 2009;94(12):1962–74.
[48] Zhu B, Frangopol DM. Reliability assessment of ship structures using Bayesian updating. Eng Struct 2013;56:1836–47.
[49] Ni YQ, Wang YW, Zhang C. A Bayesian approach for condition assessment and damage alarm of bridge expansion joints using long-term structural health monitoring data. Eng Struct 2020;212:110520.
[50] Diebolt J, Robert CP. Estimation of finite mixture distributions through Bayesian sampling. J Roy Stat Soc: Ser B (Methodol) 1994;56(2):363–75.
[51] Gelfand AE, Hills SE, Racine-Poon A, Smith AF. Illustration of Bayesian inference in normal data models using Gibbs sampling. J Am Stat Assoc 1990;85(412):972–85.
[52] Bishop CM. Pattern recognition and machine learning. New York, NY: Springer; 2006.
[53] Chib S. Marginal likelihood from the Gibbs output. J Am Stat Assoc 1995;90(432):1313–21.
[54] Melchers RE, Beck AT. Structural reliability analysis and prediction (third edition). Hoboken, NJ: John Wiley & Sons; 2017.
[55] Wang X, Ni YQ, Lin KC. Comparison of statistical counting methods in SHM-based reliability assessment of bridges. J Civil Struct Health Monitor 2015;5(3):275–86.
[56] Wong KY. Stress and traffic loads monitoring of Tsing Ma Bridge. Proceedings of the China Bridge Congress 2007, Chongqing, China, 2007.
[57] Chatterjee S. The design of modern steel bridges. Oxford, UK: Blackwell Science; 2008.
[58] Frangopol DM, Kong JS, Gharaibeh ES. Reliability-based life-cycle management of highway bridges. J Comput Civil Eng (ASCE) 2001;15(1):27–34.